



Calhoun: The NPS Institutional Archive DSpace Repository

Theses and Dissertations

1. Thesis and Dissertation Collection, all items

1950-06

Vertical motions and their relationship to the jet stream.

LaCava, John

Monterey, California. Naval Postgraduate School

<http://hdl.handle.net/10945/24882>

Downloaded from NPS Archive: Calhoun



<http://www.nps.edu/library>

Calhoun is the Naval Postgraduate School's public access digital repository for research materials and institutional publications created by the NPS community.

Calhoun is named for Professor of Mathematics Guy K. Calhoun, NPS's first appointed -- and published -- scholarly author.

Dudley Knox Library / Naval Postgraduate School
411 Dyer Road / 1 University Circle
Monterey, California USA 93943

VERTICAL MOTIONS AND THEIR
RELATIONSHIP TO THE JET STREAM

BY
JOHN LACAVA, JR.

717
THESIS

Library
U. S. Naval Postgraduate School
Annapolis, Md.

VERTICAL MOTIONS AND THEIR RELATIONSHIP TO THE JET STREAM

by
J. LaCava, Jr.

VERTICAL MOTIONS AND THEIR RELATIONSHIP TO THE JET STREAM

by
John LaCava, Jr.
Lieutenant, United States Navy

Submitted in partial fulfillment
of the requirements
for the degree of
MASTER OF SCIENCE
IN AEROLOGY

United States Naval Postgraduate School
Monterey, California
1950

This work is accepted as fulfilling
the thesis requirements for the degree of

MASTER OF SCIENCE
IN AEROLOGY

from the
United States Naval Postgraduate School

PREFACE

This paper presents the results of a study of the large scale vertical motions in the earth's atmosphere during a continuous sequence of seven days at 12-hour intervals along a specific meridian in a relatively dense radiosonde network. The objectives were threefold; first, to compute and plot cross sections of these values of vertical motions; second, to determine qualitatively the inter-relationship of the three components of the individual change of temperature at a given station; and lastly, to investigate the dynamic aspects of these vertical motions.

Undertaken as the thesis requirement for the degree of Master of Science in Aerology, this paper was prepared at the U. S. Naval Postgraduate School, Monterey, California, during the academic year 1949-1950.

The author is particularly indebted to Associate Professor Frank L. Martin of the Aerology Department for his advice and guidance during the investigation, and to the author's wife for her assistance in the laborious task of plotting and recording data.

TABLE OF CONTENTS

	Page
CERTIFICATE OF APPROVAL	i
PREFACE	ii
TABLE OF CONTENTS	iii
LIST OF ILLUSTRATIONS	iv
TABLE OF SYMBOLS AND ABBREVIATIONS	v
CHAPTER	
I. INTRODUCTION	1
II. THEORETICAL CONSIDERATIONS	3
III. TECHNIQUE OF INVESTIGATION	6
IV. RESULTS AND CONCLUSIONS	11
RIBLIOGRAPHY	26

LIST OF ILLUSTRATIONS

	Page
Table 1. Correlation Coefficients	12
Figure 1. Typical Model of Southward Moving Jet Stream	18
Figure 2. Typical Model of Northward Moving Jet Stream	19

PLATE

(Inside back cover)

- I. Geostrophic Wind Scale
- II. Isanabatic Chart, Northward Moving Jet Stream
- III. Streamline Chart for Plate II
- IV. Isanabatic Chart, Southward Moving Jet Stream
- V. Streamline Chart for Plate IV
- VI. Isanabatic Chart for Stationary Jet Stream
- VII. Streamline Chart for Plate VI

TABLE OF SYMBOLS AND ABBREVIATIONS

c_p	Specific heat of dry air at constant pressure
g	Acceleration of gravity
GCT	Greenwich civil time
J_i	Position of jet stream center at beginning of interval
J_f	Position of jet stream center at end of interval
mb	Millibar
P_1	Pressure at bottom of layer
P_2	Pressure at top of layer
R_d	Gas constant per gram of dry air
t	Time
\bar{T}^*	Mean virtual temperature
T	Temperature
T_i	Position of tropopause at beginning of interval
T_f	Position of tropopause at end of interval
\mathbf{V}	Wind velocity vector
w	Vertical component of wind velocity
w_p	Vertical velocity of a point that moves along a constant pressure surface
ρ	Density
γ	Lapse rate of temperature
δ_d	Dry adiabatic lapse rate
∇	Vector del operator
$\nabla_u T$	Horizontal temperature gradient
Δz	Thickness between two pressure surfaces
$\frac{dT}{dt}$	Rate of change of temperature on an individual air particle
$\frac{\delta T}{\delta t}$	Rate of change of temperature of an individual air particle moving on a constant pressure surface

$\frac{\partial T}{\partial t}$ Local change of temperature

$\nabla \cdot \nabla_h T$ Horizontal temperature advection, positive for cold advection

I. INTRODUCTION

During recent years a great amount of work has been done in the methods of computation and analytical aspects of the fields of vertical motions in the atmosphere. These vertical motions are of the large scale type, with values of small magnitude, and are not to be confused with the extremes found in thunderstorms and heavy cumulus clouds. Panofsky, Miller, Fleagle and others of New York University [5], in a project sponsored by the Army Air Forces Weather Service, have published extensive material along these lines. In [5] they analyzed the fields associated with the development and dissipation of a cyclone and an anticyclone in the center of the United States. This paper attempts to deal with the vertical motions along a specific meridian; namely, the 80th meridian, and to attempt to analyze the vertical motions associated with the troughs, ridges and cyclones as they pass over the meridian.

There are several methods of computing the value of the vertical component of velocity at a point, and the reader is referred to [4], [5] and [8]. The methods may be broken into two main types, Kinematic and Adiabatic. Although Kinematic types yield instantaneous vertical velocities, they are difficult to apply because observed winds must be used, and, as a general rule, these are not available consistently at high elevations. Adiabatic techniques yield average vertical velocities over the period of time used in the computation, and can be computed at regions and elevations where wind data is sparse. In [5] the authors have computed the vertical velocities for one situation by several different techniques, and have concluded that the different methods give results of the same sign but

slightly varying magnitudes. Since constant pressure charts were to be used at the various levels, the isobaric technique as given in Chapter II was chosen.

In [2] Fleagle has deduced the three-dimensional fields of vertical motions in relation to a selected cyclone and anticyclone. These pressure systems were both characterized by flat troughs and ridges aloft. In this study the author has concentrated on the problem of the two-dimensional field of vertical motion along the 80th meridian, west longitude. The synoptic situation selected for the present study was also characterized at upper levels by flat ridges and troughs, and in the case of the cyclones, there was also agreement with Fleagle's case study in that a well marked frontal system existed at the surface in all cases. It is therefore not surprising that all statistical relationships deduced herein between vertical velocities and other mechanisms of temperature change are in qualitative agreement with those of Fleagle.

In addition to the foregoing statistical results, the author attempted to correlate the fields of vertical motions with the movement of the fronts at the 500 mb level and the jet stream axis along the 80th meridian, paying close attention to pressure changes. It was possible to deduce a dynamic model of the mean vertical and cross isobar circulations in the vicinity of the jet for both northward and southward moving jets.

II. THEORETICAL COMPUTATIONS

The isobaric technique as described by Panofsky [8] was used in the computations of vertical velocities. Using the notations as listed in the table of symbols, the individual change of temperature of a moving air particle may be written

$$\frac{dT}{dt} = \frac{\partial T}{\partial t} + \mathbf{V} \cdot \nabla_H T + w \frac{\partial T}{\partial z} \quad (1)$$

since

$$\frac{dT}{dt} = \frac{dT}{dz} \frac{dz}{dt} = w \frac{dT}{dz}$$

equation (1) may then be written

$$\frac{\partial T}{\partial t} + \mathbf{V} \cdot \nabla_H T + w \left(\frac{\partial T}{\partial z} - \frac{dT}{dz} \right) = 0. \quad (2)$$

From the First Law of Thermodynamics

$$c_p dT = \frac{1}{\rho} dp$$

Multiplication of both sides by $\frac{w}{dz}$ gives

$$w c_p \frac{dT}{dz} = w \frac{dp}{dz}$$

Since $w \frac{dp}{dz}$ is approximately equal to $w \frac{\partial p}{\partial z}$ which is equal to $-g\rho w$

$$-w \frac{dT}{dz} = w \frac{g}{c_p} = w \gamma_d.$$

(3)

Equation (2) may then be written,

$$\frac{\partial T}{\partial t} + \mathbf{v} \cdot \nabla_H T + w (\gamma_d - \gamma) = 0 \quad (3)$$

The individual change of temperature of a particle following a constant pressure surface is given by

$$\frac{\delta T}{\delta t} = \frac{\partial T}{\partial t} + \mathbf{v} \cdot \nabla_H T + w_p \frac{\partial T}{\partial z} \quad (4)$$

Subtracting (3) from (4), one obtains

$$\frac{\delta T}{\delta t} = -w (\gamma_d - \gamma) + w_p \frac{\partial T}{\partial z} .$$

According to Panofsky [9], w is in magnitude 10 times greater than w_p , therefore the latter may be neglected, giving the final equation

$$w = - \frac{\frac{\delta T}{\delta t}}{\gamma_d - \gamma} . \quad (5)$$

The terms on the right hand side of this equation can then be evaluated with the use of data obtained from constant pressure maps and cross sections. Assuming that the contours on the constant pressure maps are streamlines, and that no radical change of flow pattern occurs, the trajectories of an air particle arriving at a given station can be computed. The lapse rate term is computed from the cross section data.

The use of this formula depends on the assumption of adiabatic motion, that is, if any temperature change is observed in the trajectory of the air particle, it was due to cooling or heating in an adiabatic process. For the most part, especially at 500 and 300 mbs, this has not been too serious a requirement because: (a) the moist adiabatic lapse rate closely approximates the dry adiabatic; (b) solar heating and cooling effects have been eliminated from the observed parcel temperature change (see page 8). Such other non-adiabatic effects as turbulent transport of water vapor and long wave radiation from the earth have been assumed small and no further corrections were made. Using finite differences as explained in Chapter III., the vertical motions were computed at the 700, 500 and 300 mb levels.

III. TECHNIQUES OF INVESTIGATION

The synoptic situation desired for this investigation was one in which the polar front was far enough south so that the jet stream would make its appearance somewhere in the northern United States, in the area where the radiosonde network was sufficiently dense to obtain consistent reports for the analysis. The second requirement was that a series of migratory systems would pass over the meridian during the period of the investigation. These requirements seemed to be best fulfilled from data available, along the 80th meridian during the interval from 22 January 1949 to 27 January 1949. Prior to this time the polar front had been steadily moving south, and, at the beginning of the period, was situated as a stationary front just south of Charleston, South Carolina. During the period a series of migratory anticyclones and developing waves on the polar front alternately passed the meridian.

The first phase of the compilation of the data consisted of the plotting and analyzing of the 700, 500 and 300 mb charts and vertical cross sections along 80° W. longitude. All charts were analyzed twice daily, at standard radiosonde times, 0300 and 1500 GCT. The constant pressure charts were analyzed with contours for every two hundred feet, and isotherms for every two degrees centigrade. The cross sections were analyzed to obtain the location of the frontal surface in the vertical, and to locate the center of the jet stream. In analyzing the cross sections the use of mixing ratio, isotherms, isentropes, and observed winds were applied in the conventional manner for frontal analysis. The west wind component was computed from the

actual reports of the observing stations and a specially prepared graph (Plate I) for determining the geostrophic wind from the slope of the pressure surface. Since the cross sections were oriented exactly north-south, any computation of geostrophic wind between two stations is automatically a west wind component providing the elevation of the constant pressure surface is decreasing toward the north. If it is increasing toward the north, then the computation from the graph gives an east wind component.

In computing the trajectories, the assumption was made that the contours were streamlines. Secondly, it was assumed that the wind was geostrophic. This assumption was quite valid in this case, as, in the entire period studied, the flow aloft in the regions where the trajectories were to be computed showed very little curvature, tending to make the gradient wind nearly equal to the geostrophic wind. Furthermore, Neiburger [7] has shown that the deviation of the computed gradient wind was as great as the deviation of the geostrophic wind from the observed wind. The trajectories were taken over a twelve hour period, using a method of second approximations. The measured geostrophic wind was projected upwind for a period of six hours. At this point the wind was again measured and projected upwind at this speed for another six hours. The point was then marked on the previous map and projected downwind in the same manner. From the downwind trajectory, a resultant trajectory can be computed, which, when applied to the starting point, should present the approximate trajectory of the particle in arriving at the given station. It is felt that this method gives more accuracy in the

upper levels, where the gradient may change considerably over the period of the trajectory, than a simple upwind projection of the measured wind at the starting point. Ideally the station at which the vertical velocity is desired should be at the midpoint of the trajectory, but along the 80th meridian several trajectories would terminate over ocean areas where reasonable interpolation of temperature is not possible.

With the establishment of the trajectories, the increment of temperature change is found. Since the computation of vertical velocity rested to such a great extent on this value, the question of diurnal variation of temperature following the particle arose. In [5] Miller et al computed from a large number of reports, the diurnal temperature corrections at times which applied to this problem. These corrections were as follows: at 700 mb, $\pm .3^{\circ}$ C; at 500 mb, $\pm .8^{\circ}$ C; at 300 mb, $\pm 1.5^{\circ}$ C. The plus sign applies for any trajectory computed between 0300-1500 GCT, while the negative sign applies for trajectories terminating at 0300 GCT. These corrections were subtracted from the increment of temperature obtained from the trajectories before the vertical velocities were computed.

To determine the existing lapse rate γ in [5], the arithmetic mean of the lapse rate at the beginning and end of the time interval was used. The observed temperature at the mandatory radiosonde level above and below that for which the computation is being made was divided by the distance between the two levels as prescribed by the U. S. Standard Atmosphere. With the evaluation of the lapse rate term, the values of vertical motion can be computed. During the computations of the trajectories, it was observed that in regions north of Moosonee (836) and south of Charleston (208), the end

point of trajectories usually were in areas where reasonable interpolation was impossible. Accordingly, the investigation was limited to the following six stations: Charleston (208), Greensboro (317), Pittsburgh (520), Buffalo (528), Sault St. Marie (734) and Moosonee (836). It is repeated here for emphasis, that since a twelve hour trajectory was used in computing the temperature difference of the particle of air, the vertical motions represent an average over this period. Any extremes of rising or falling motion that have occurred in the period tend to be damped out, and the resultant average vertical velocities usually fall in the range of 0 to $\pm 5 \text{ cm sec}^{-1}$.

With the assumption that the term w_p is negligible, the individual change of temperature of a particle following a constant pressure surface can be written

$$\nabla \cdot \nabla_H T = \frac{\partial T}{\partial t} - \frac{\partial T}{\partial t} \quad (6)$$

where $\frac{\partial T}{\partial t}$ represents the local change of temperature observed at the station, and $\nabla \cdot \nabla_H T$ represents the component due to horizontal advection. The value of $\frac{\partial T}{\partial t}$ is easily obtained from the constant pressure charts, while the value of $\frac{\partial T}{\partial t}$ is the temperature change, with non-adiabatic effects eliminated, and was computed from the trajectories. The value thus obtained from (6) represents the advective component. Since the inter-dependence of the variates in equation (3) were not clearly visible, it was decided to correlate combinations of these variates in an effort to determine the sign, magnitude, and

variability of the relationship with height. The use of correlations in this study was rather to determine the relationship between variables than to try to formulate any regression equation for forecast uses. Accordingly, the variables were correlated at each of the three levels for which computations were made, and the results of these correlations were used in a qualitative manner in the analysis of the fields of vertical motions.

The frontal structure, jet stream center, and computed vertical motions were transferred to fresh charts of the same scale. The movement of the jet centers was well marked in the horizontal plane, but due to lack of reports at high levels, the vertical movement of the jet is subject to considerable question, hence no attempt will be made to explain the latter.

*Isanabats of vertical velocity were drawn and the data prepared for analysis.

* Lines of equal vertical velocity.

IV. RESULTS AND CONCLUSIONS

The computations of vertical velocities were carried out for 224 cases, approximately 75 cases for each level. Certain observations were ruled out when the initial point of the trajectory fell in regions where reasonable extrapolation of temperature could not be made due to lack of reports.

For determining the inter-relationship of the variates, equation (3) of Chapter I was chosen. All terms of this equation had been evaluated according to methods described in Chapter II, therefore, applying certain assumptions to equation (3) it is possible to obtain qualitative results of the variates. Using vector notation a positive value of $\mathbf{W} \cdot \nabla_{\mathbf{H}} T > 0$ represents cold advection. Since the term $(\delta d - \gamma)$ is always positive, the sign of the entire term $w(\delta d - \gamma)$ is determined by the sign of w . Upward vertical motions were chosen as positive, and downward motions as negative. The results of the correlations are listed in Table 1.

Set A. Vertical Motions and Advection. If in (3) we assume that there is a level where the local change of temperature is small, then the advective term and the vertical motions term should be approximately equal and opposite in sign for (3) to be valid. If local change were assumed exactly zero, and advection and vertical motions exactly balanced each other, the correlation coefficient would be -1.0. From this we may conclude that in the region where the magnitude of the correlation coefficient is greatest, the assumption is most nearly valid.

CORRELATION COEFFICIENTS

(A)

$$w(\gamma_d - \gamma), \quad W \cdot \nabla_H T$$

300 mb - .68

500 mb - .50

700 mb - .41

(B)

$$\frac{\partial T}{\partial t}, \quad W \cdot \nabla_H T$$

- .48

- .55

- .58

(C)

$$w(\gamma_d - \gamma), \quad \frac{\partial T}{\partial t}$$

300 mb - .28

500 mb - .32

700 mb - .44

(D)

$$\frac{\partial \theta}{\partial t}, \quad w$$

- .51

- .21

- .33

(E)

$$\frac{\partial P}{\partial t}, \quad w$$

300 mb .09

500 mb - .12

700 mb - .41

TABLE 1.

Actual results show negative correlation coefficients increasing in magnitude and with height. The negative coefficients show that cold advection is accompanied by downward motions. From the magnitude of the coefficients, it can also be said that this compensation is greatest at high levels. This is in good agreement with Fleagle's results [2].

Set B. Local Change of Temperature and Advection. From (3) if one assumes the vertical motion term is small, then advection and local change of temperature should be opposite in sign. The negative correlation coefficients indicate that for $\nabla \cdot \mathbf{V}_H T > 0$, $\frac{\partial T}{\partial t} < 0$. This states as expected, that cold advection is accompanied by local cooling. In interpreting the magnitude of the correlation coefficients as explained above, we may say that the assumptions of small vertical motions is most nearly met in the lower troposphere, and that vertical motions increase with height. This also implies that advection is predominant in the lower troposphere and decreases with height, which is again in good agreement with Fleagle's ? results [2].

Set C. Local Change of Temperature and Vertical Motions. From (3), if one assumes that advection is small, then the vertical motion term and local change of temperature term should be opposite in sign and approximately equal. The negative correlation coefficients verify the opposing sign requirement, indicating that with local warming $\frac{\partial T}{\partial t} > 0$, there are downward motions $w(\gamma_d - \gamma) < 0$. From the change of magnitude of the correlation coefficients with height, it is indicated that the assumption of advection being small is best met in the lower troposphere, and that advection increases with height. This also implies that vertical motions

are more predominant at lower than at higher levels. These qualitative results are opposed to those obtained from Set B. It is to be noted that the magnitude of the coefficients in Set C. are in all cases smaller than either Sets A. or B., indicating less reliability through possible scattering of data.

Set D. Local Change of Potential Temperature and Vertical Motions. The values of $\frac{d\theta}{dt}$ were computed from values of temperature at the beginning and end of the interval. Since these in turn were computed directly from the local values of temperature change, it would appear that since vertical motions are being correlated with $\frac{d\theta}{dt}$, the level where the correlation coefficient is greatest indicates the region where vertical motions are predominant. The negative coefficients obtained indicate, as expected, that local increase of potential temperature ($\frac{d\theta}{dt} > 0$), is associated with downward motions. The magnitudes of the coefficients seem to indicate agreement with the results obtained in Set B; namely, that vertical motions assume greater prominence than advection in the region of 300 mb.

Set E. Surface Twelve Hour Pressure Tendency and Vertical Motions. In the lower levels the sign of the coefficients indicate that increasing pressure is accompanied by downward motions in the lower troposphere. The reversal of the sign of the coefficient with height indicates that at some upper level rising surface pressure is correlated with upward motions. The magnitude of the coefficients above 700 mb are small; the definite decrease, however, indicates the classical vertical motion model drawn above cyclones and anticyclones.

The twelve hour surface tendencies were plotted at the top of the isanabatic charts. (See Plates II, IV, and VI). In general the results were gratifying. The regions of greatest surface pressure tendencies were usually located over the regions of strongest vertical motions. The correspondence was most pronounced where the vertical motions extended to 300 mb without a change of sign. Plate IV shows a maximum negative tendency over Greensboro and upward motions at all levels. The maximum positive tendency occurs at Sault St. Marie, just north of the field of downward motions. Plate VI shows practically a one-to-one correspondence between the locations of the maximum ascending and descending currents and those of the corresponding surface pressure tendency centers. Here all vertical motions extend to 300 mb without a change of sign.

During the period investigated, one cyclonic center of moderate intensity developed in the lower Mississippi Valley. This system moved on a northeasterly course toward Pittsburgh. The effect of the movement of this system on the level of non-divergence in the Pittsburgh area was interesting to note. From the tendency equation, in a manner shown by Palmen [13], it can be shown that the level of non-divergence is approximately at the level of maximum ascending or descending motion, providing that the local change of pressure is zero. Since the latter statement is approximately true, (Fleagle [2]), the mass transport through the level in question must be equal to the divergence occurring above that level. In the instance mentioned above, the level of non-divergence fell from about 400 mb to approximately 650 mb in an interval of twelve hours, followed by a rapid deepening in the Pittsburgh

area in the next twelve hours. From the enclosed Plates, it can also be seen that there are possibly two levels of non-divergence, one in stratospheric levels and the one normally referred to at mid-tropospheric levels.

Concerning the statistical work in general, it may be said that the results are in good agreement with those of Fleagle, Miller and others. Hence, it seems plausible that further relationships, as derived by Fleagle in regions not investigated in this paper, will be applicable in this situation.

The initial problem in the analysis of the fields of vertical motion was to determine a criterion, in the light of already established results, that the vertical motions might be expected to follow. Namias [6] states that the steep slope or break of the tropopause surface directly above the jet stream is one factor that must be explained in any plausible complete theory of this phenomena. In the studies of Palmen [9] [10] [11], and in the cross sections used in this study, it was noted that the tropopause was at a minimum height just north of the jet stream, and that just north of that minimum, its height increased slightly. South of the jet stream the tropopause appeared at its highest level. By using the thermal wind equation as suggested by Namias [6], it can be proved that in general, the most strongly sloping portion of the tropopause surface must pass through the axis of the jet stream, for, at this point the rate of change of the geostrophic wind with height is zero, hence the horizontal thermal gradient and vertical lapse rate both become very small or zero, indicating the location in the vertical of the tropopause region. Assuming no discontinuity in the tropopause, it can then be

drawn as illustrated in Figures 1 and 2. Consequently if the center of the jet moves to the south, then the tropopause must move to the dashed line positions in Figures 1 and 2. Even if one considers the possibility of a discontinuity in the tropopause just south of the jet, then there must be some mechanism to create a lower tropopause when the jet is moving south, and one to destroy it when the jet is moving north.

As has been stated before, the synoptic situation was one in which there were no marked pressure systems, but rather a polar front with a series of waves passing the meridian. Consequently, the conventional notation of a cold front or warm front as the movement of the frontal surface on the surface of the earth was equally indistinct and did not indicate any correspondence with the movement of the jet stream center. Palmen [11] states

Often it is not possible to connect minor disturbances at the surface with the band of strong isotherm concentration at 500 mb, but large scale displacement of surface fronts can usually be related to similar displacements aloft.

He further states that empirical data point to the fact that the jet stream is located directly over the layer of maximum temperature gradient at 500 mb. As an aid in locating this region of maximum temperature gradient, the following method was used. From the integrated form of the hydrostatic equation, the thickness of the layer between the constant pressure surfaces P_1 and P_2 is given by

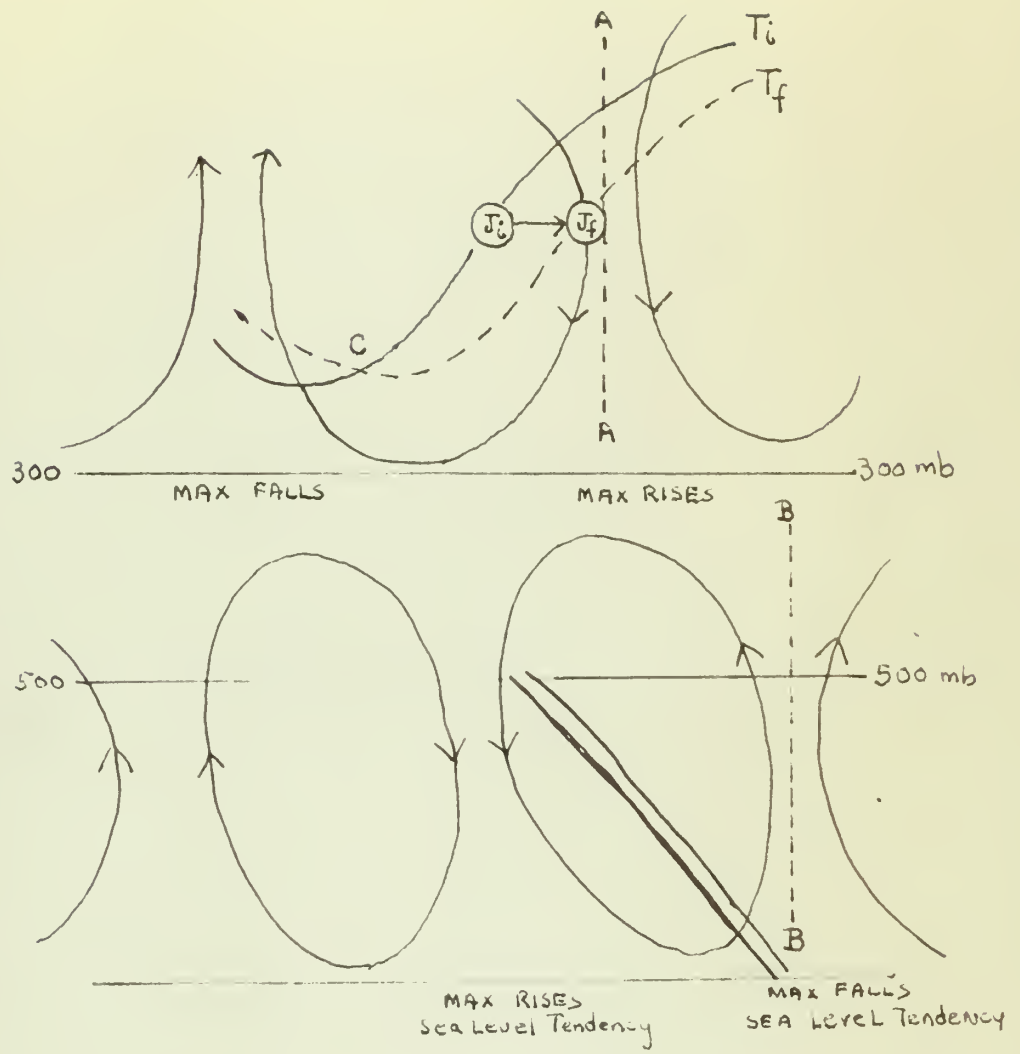
$$\Delta z = \frac{R_d}{g} \bar{T}^* \left(\ln \frac{P_1}{P_2} \right) = K \bar{T}^*$$

where

$$K = \frac{R_d}{g} \left(\ln \frac{P_1}{P_2} \right)$$

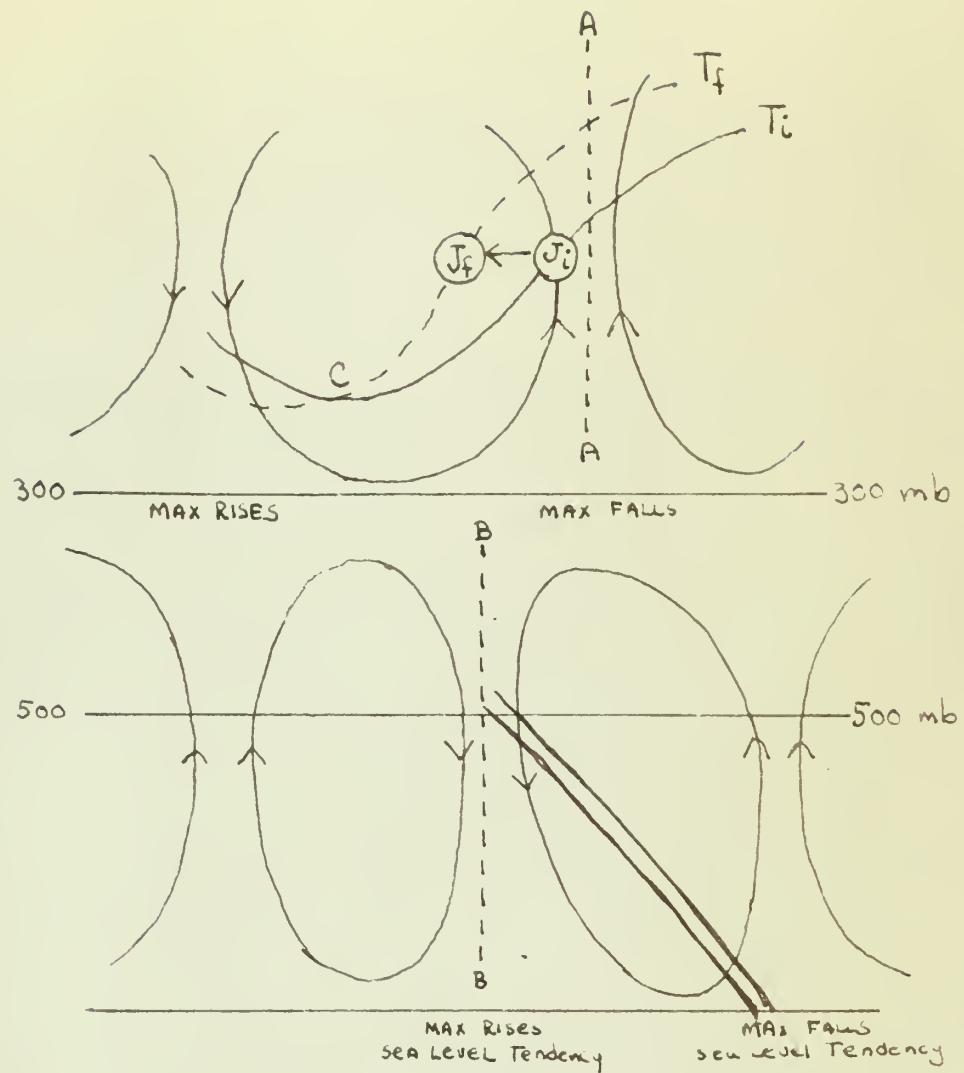
Differentiating with respect to time

$$\frac{\partial}{\partial t} (\Delta z) = K \frac{\partial \bar{T}^*}{\partial t}$$



SOUTHWARD MOVING JET

Figure 1.



NORTHWARD MOVING JET

Figure 2.

or the rate of change of thickness of a specific layer in a specific time interval is directly proportional to the rate of change of mean virtual temperature in the same interval. Entering these values on the cross section made it quite simple to pick the band of strongest temperature gradient in the layer between 500 and 700 mb. This criterion made it possible to verify Palmen's relationship between the jet stream and the polar front at 500 mb, in that, with the maximum gradient of temperature in the layer shifting to the south, the jet stream also shifted to the south.

Since the tropopause is the point in the atmosphere where the lapse rate becomes small and approaches isothermal conditions,* it is reasonable to believe that vertical motions and their associated adiabatic heating and cooling might supply the reason for the lowering and raising, creation or destruction of the tropopause in the situations mentioned above. Using this as a basis, two tentative vertical motion models can be drawn, Figures 1 and 2. These models are essentially similar to those proposed by Palmen [11]. In Figure 1, for example, the point C, which represents the point of intersection of the two consecutive tropopause surfaces, (12 hours apart), must represent the point of zero mean vertical velocity. It is to be noted that the vertical motions shown in Figures 1 and 2 represent mean vertical motions for a 12-hour period ending with the given time, and therefore account for a movement of the jet from J_i to J_f . The meaning of the circulation axes AA and BB is discussed on pages 24 and 25.

The vertical circulation models of Figures 1 and 2 below the 300 mb level can in general be identified with rising or falling surface pressures.

* According to Penndorf and Flohn [13], $\gamma = .2$

This follows from the correlations of Table 1 and is verified by Fleagle [2], pp. 183-184, who states

Upward motions occurred in regions of pressure fall and downward motions occurred in regions of pressure rise, and the vertical components were approximately proportional to the pressure changes.

This tendency has already been noted earlier on page 15.

The next step is to verify the fields of vertical motions of Figures 1 and 2 above 300 mb. Although vertical motions were not computed above 300 mb in this study, the results of Fleagle's study [2] were drawn upon, and, in addition, strong consideration was given to the 300 mb height tendency during the previous twelve hours. It was quite easy to distinguish on all cross sections the areas of maximum twelve hourly rise and fall of the 300 mb surface. Since this surface is quite close to the stratospheric levels considered by Fleagle, it is assumed that a large contribution of the twelve-hourly height change at 300 mb is due to the layer between 9 and 16 kilometers, (300 to 100 mb). Fleagle also noted that this layer contained the maximum temperature advection for the atmosphere, at least to the levels considered, and that temperature advection also tends to be systematically compensated by vertical motions at these levels. In the light of the foregoing, it was assumed that the region of maximum height change at 300 mb indicates the location of maximum advection above 300 mb, which in turn, indicates the maximum values or "chimneys" of the mean vertical motions. Thus a region of maximum positive height tendency is experiencing strong cold advection and compensating downward motions, with an analogous statement for negative tendencies.

It has been noted in the previous paragraph how the maximum height tendencies at 300 mb determine the vertical motion fields above this level, and in particular, the areas of maximum ascent and descent. This mechanism will now be correlated more closely with the models of Figures 1 and 2. The final results of the analysis of the cross sections in the period studied showed that, according to the convention of thermal gradient discussed above, there were six instances of the northward moving jet, three of the southward moving jet, and three of the stationary jet. Plates II, IV, and VI illustrate the vertical motion field, frontal structure and the jet stream for a typical situation of each of the above types. Plates III, V, and VII are corresponding charts of streamlines drawn from the plotted and estimated vertical motion fields. On the isanabatic charts, the numbers appearing at the significant levels 700, 500, and 300 mb represent the height tendency of the surface during the previous twelve hours. The numbers appearing midway between the significant levels are those of thickness tendency between the two levels during the past twelve hours.

Plates II and III are typical illustrations of a northward moving jet stream. At low levels the frontal surface had progressed southward, but at the 700-500 mb layer the maximum thermal gradient had shifted poleward. This indicated a gradual reduction of the slope of the frontal surface in a manner described by Crocker et al [1] in the article on frontal contour charts. In all cross sections of this category, there occurred either (i), a combination of maximum rises north, maximum falls south of the initial position of the jet, or (ii), the same relative gradient of height tendency at the

300 mb level as indicated in (i). It appears that the southward directed tendency gradient has the effect of wiping out the jet at the lower latitude position and thus shifting it northward. However, it was difficult to reconcile the observed amount of jet movement on the cross section with the observed height tendencies at 300 mb.

Plates IV and V are typical examples of a southward moving jet. This type of jet occurred with 300 mb height tendency falls to the north of the jet and rises to the south, in such a manner that the horizontal pressure gradient was increased southward relative to the initial position of the jet.

Plates VI and VII are illustrations of the situation in which the movement of the jet was small enough to be termed "stationary". The north-south distribution of height tendencies at 300 mb was analyzed as before. The notable feature in these types was that the vertical motion fields usually persisted to high levels without a change of sign. The stationary types observed had the vertical circulations of the southward moving type, indicating the possibility that, although the movement of the jet was not large enough to definitely show up in the analysis, it corresponded apparently to the southward moving type in this instance.

Thus, in Figures 1 and 2 the areas of maximum rises and falls have been indicated in their proper position relative to the jet. Introducing next the appropriate upper level vertical circulations which these centers of rising and falling tendencies imply, it is seen that the vertical motions are also consistent with the observed tropopause movements. The vertical

circulation models presented in Figures 1 and 2 therefore fit all of the observed data of this and Fleagle's study and may be taken to represent a tentative vertical circulation pattern in relation to cold and warm fronts at the 500 mb level. Further study will be necessary before any conclusive verification of Figures 1 and 2 may be said to have been achieved.

It should be emphasized that this study dealt only with cases in which there were no closed circulations at upper levels in the region studied. The frontal structures, however, were quite well marked. There remains the question of explaining the occurrence of dynamic instability with the attendant cut-off lows and highs which result when instability occurs. Palmen [11] has studied a case of dynamic cyclogenesis and attributes the development of a closed vortex above 300 mb essentially to the fact that the upper level axis AA of Figure 1 has become collinear with the lower level circulation axis BB. Similarly in Figure 2, dynamic anticyclogenesis would occur when the vertical circulation axis AA, typical of rising pressure at upper levels, becomes collinear with the axis BB, typical of rising pressure in the lower tropospheric levels. Such a case had been discussed by Wexler [13].

The answer to the question of dynamic instability probably lies in the fact that such cases usually occur when surface frontal characteristics are weak or non-existent, and the amount of advection at all levels becomes quite small. In the latter case, it therefore seems likely that the vertical motions could be governed mainly by the three-dimensional

divergence or convergence above 300 mb. With slight advection it seems that the amount of divergence aloft in the vicinity of axis AA of Figure 1 could increase, causing an increased downward circulation and warming at 300 mb. This would cause a lowering tropopause and ultimately a closed low at 300 mb. The diminishing pressure under AA then causes the lower atmospheric circulation pattern BB to shift under AA.

As in any statistical investigation in which a small number of cases is used, care must be taken before formulating final conclusions. The general agreement between cases, however, was quite well-marked, indicating that further study along the same lines is warranted. Investigations using one of the other techniques for computing vertical motions as listed in [4] [5] [8] would be an excellent criterion for comparison.

BIBLIOGRAPHY

1. Crocker, A. M., N. L. Codson, and C. W. Penner. Frontal Contour Charts. *Journal of Meteor.*, 4: 95-99, June 1947.
2. Fleagle, Robert G. The Fields of Temperature, Pressure and Three Dimensional Motion in Selected Weather Situations. *Journal of Meteor.*, 4:165-185, December 1947.
3. Fleagle, Robert G. A Study of the Effects of Divergence and Advection on Lapse Rate. *Journal of Meteor.* 3:9-13, March 1946.
4. Miller, James. Applications of Vertical Velocities to Objective Weather Forecasting. Department of Meteorology, New York University. (Timeographed) 1946.
5. Miller, James E. A Study of Vertical Motion in the Atmosphere. Department of Meteorology, New York University. (Timeographed) 1946.
6. Namias, J., and P. E. Clapp. Confluence Theory of the High Tropospheric Jet Stream. *Journal of Meteor.* 6:330-336, October 1949.
7. Neiburger, H., I. Sherman, W. W. Kellogg, and A. F. Gustafson. On the Computation of Wind from Pressure Data. *Journal of Meteor.* 5:87-92, June 1948.
8. Panofsky, H. A. Methods of Computing Vertical Motions in the Atmosphere. *Journal of Meteor.* 3:45-49, June 1946.
9. Palmen, E., and K. V. Nagler. An Analysis of the Wind and Temperature Distribution in the Free Atmosphere over North America in the Case of Approximately Westerly Flow. *Journal of Meteor.* 5:58-64, April 1949.
10. Palmen, E., and K. V. Nagler. An Analysis of the Wind in the Upper Westerlies. *Journal of Meteor.* 5:20-27, February 1948.
11. Palmen, E., and K. V. Nagler. The Formation and Structure of a Large Scale Disturbance in the Westerlies. *Journal of Meteor.* 6:227-242, August 1949.
12. Palmen, E. Origin and Structure of High-level Cyclones South of the Maximum Westerlies, *Tellus*. 1:22-31, February 1949.
13. Penndorf, R., and H. Flohn. The Stratification of the Atmosphere. *Bulletin of the Amer. Met. Society*. 31:71-78, March 1950.
14. Wexler, H. Some Aspects of Dynamic Anticyclogeneses. University Chicago Inst. Meteor., Misc. Rep. 8, 1943.

DEC
- 28
93

Weather Bu

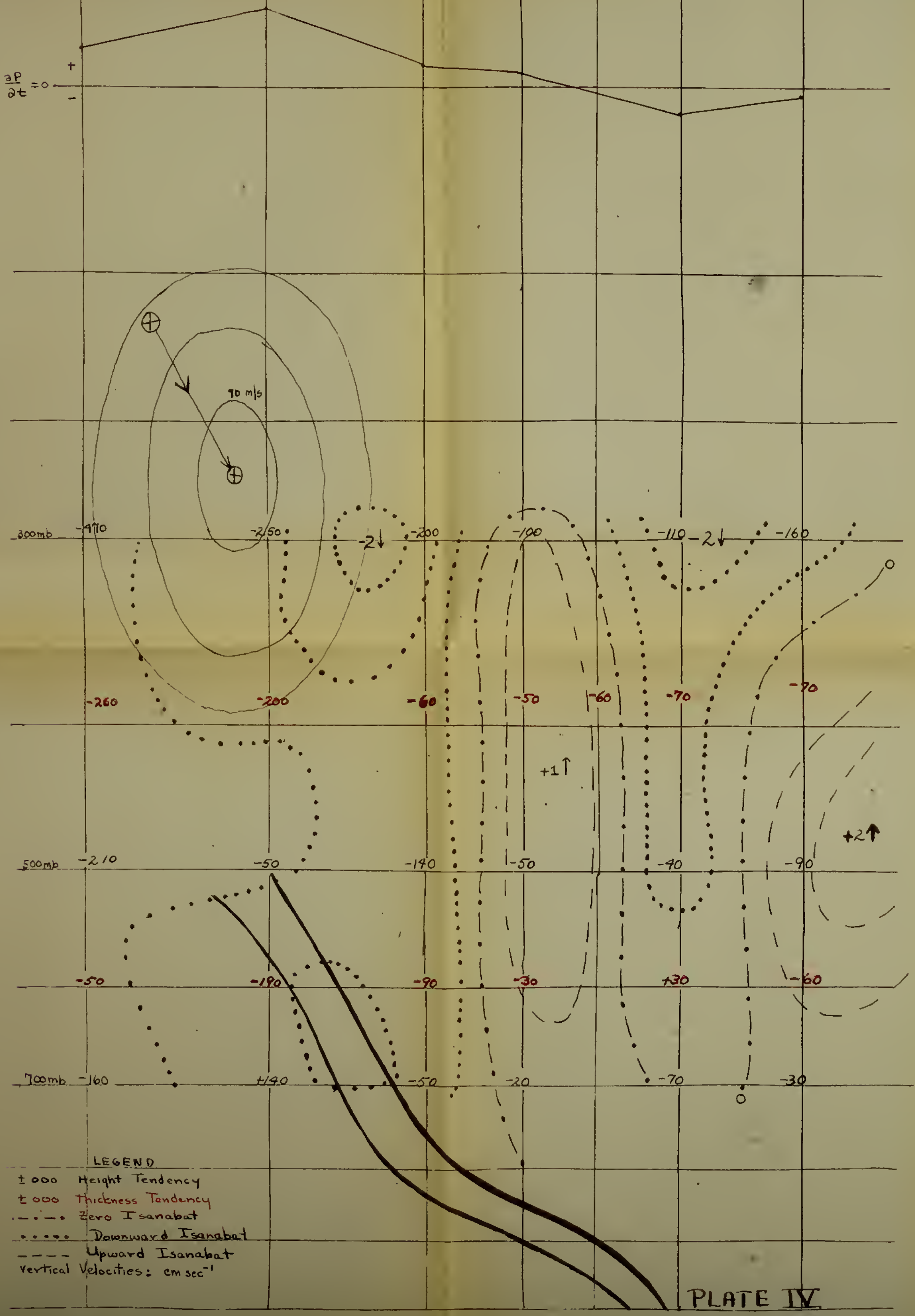
13123

Thesis
L16

LaCava
Vertical motions and
their relationship to the
jet stream

JE 9
23

INTERIM
Weather Bu



25 JAN. 1949 0300Z

200mb

J_i

J_f

300 mb

500mb

700mb

PLATE V

836
MOOSONEE

754
SHULT ST MARIE

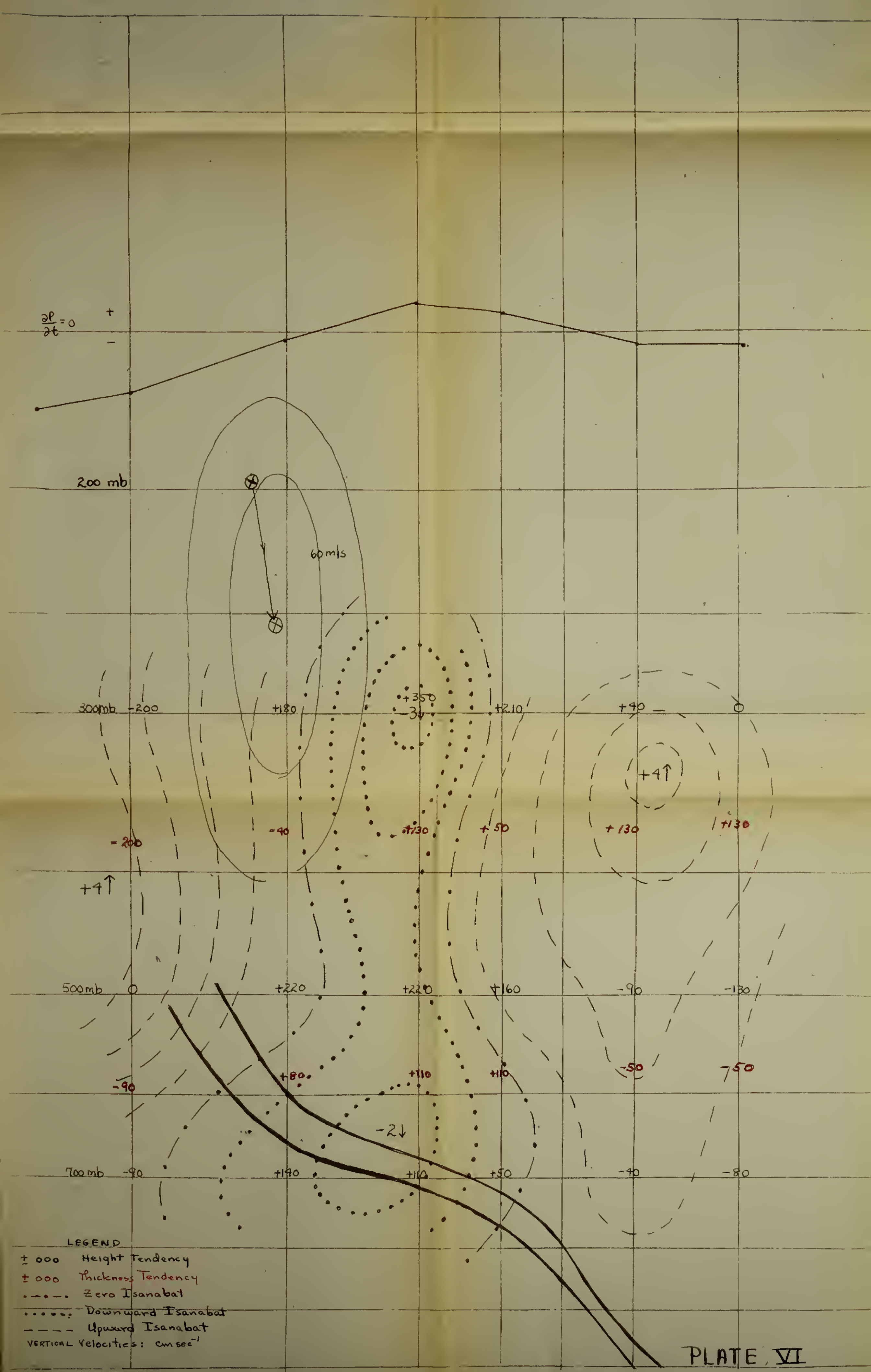
528
BUFFALO

620
PITTSBURGH HUNTINGTON GREENSBORO

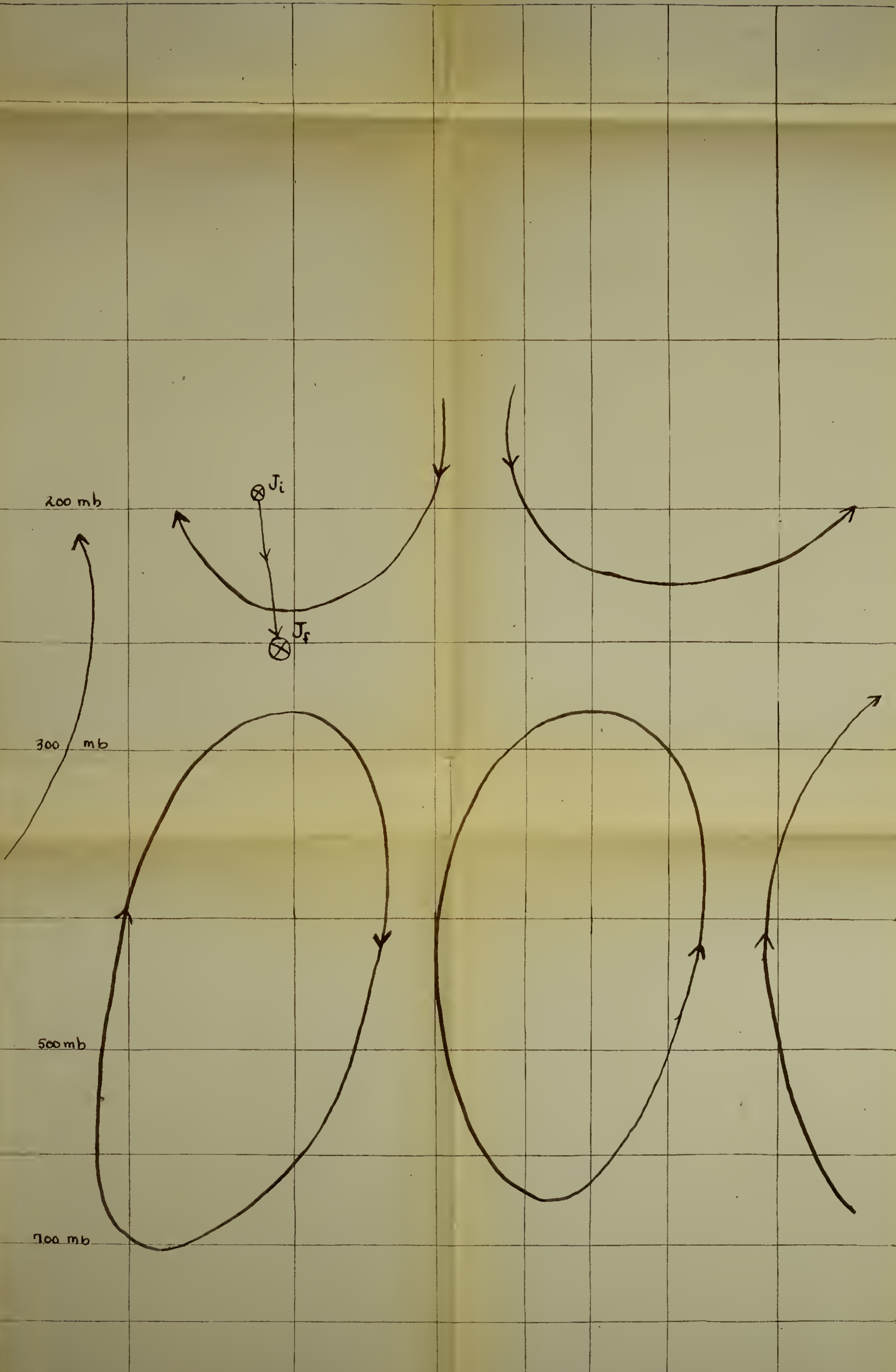
425
CHARLESTON

SOUTHWARD MOVING JET

25 JAN. 1999 0300Z



27 Jan 1949 1500Z



STATIONARY JET

PLATE VII

836
MOOSONEE

139
SAULT ST. MARIE

528
BUFFALO

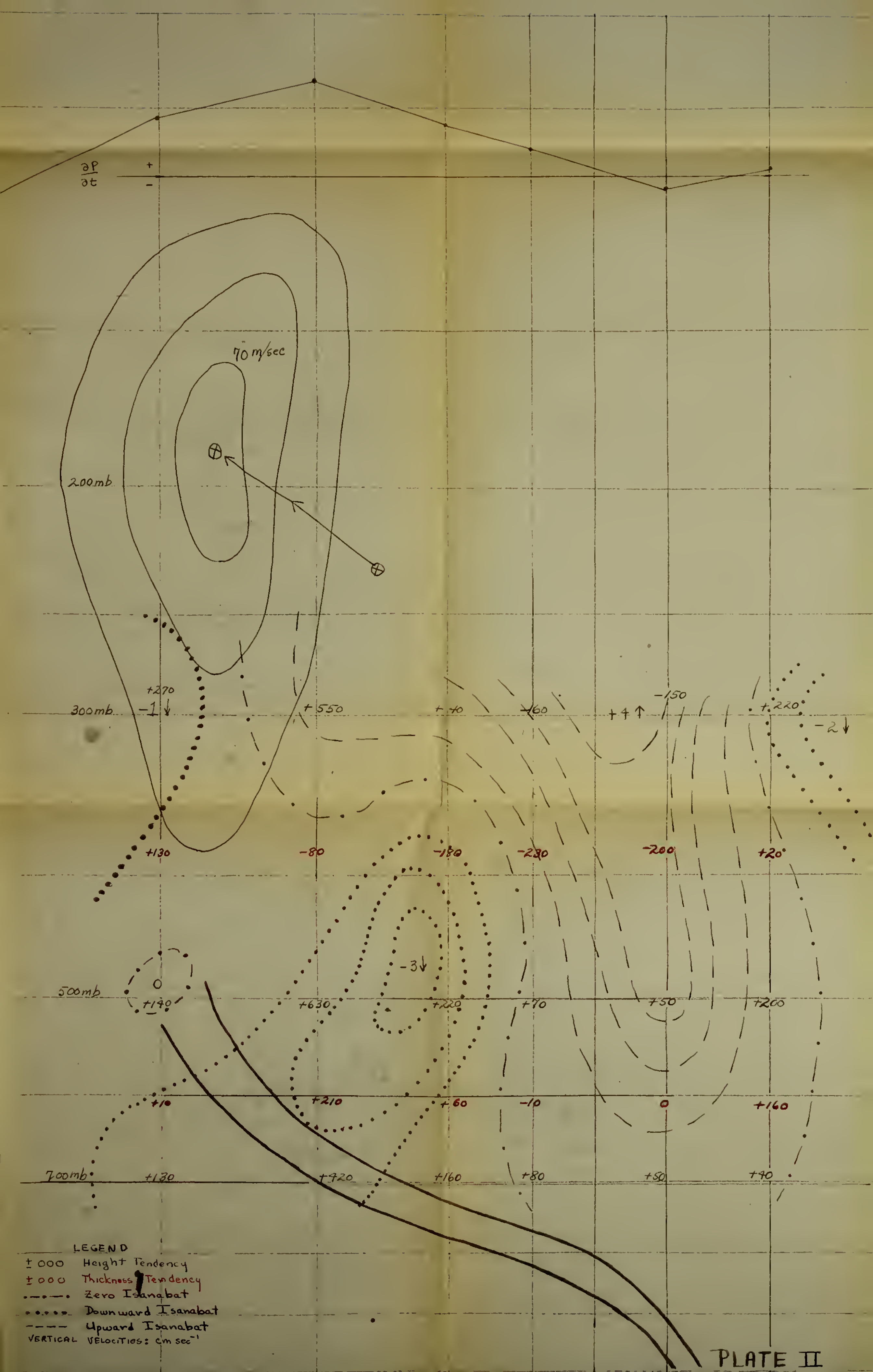
520
PITTSBURGH

925
HUNTINGTON

317
GREENSBORO

208
CHARLESTON

27 JAN. 1500 Z, 1949



LEGEND

- Height Tendency
- Thickness Tendency
- Zero Isanabat
- Downward Isanabat
- Upward Isanabat

VELOCITIES: cm sec⁻¹

PLATE II

836

134

528

520 925 317
PITTSBURGH HUNTINGDON GREENWOOD

208

NORTHWARD MOVING JET

22 JAN 1949 1500 Z

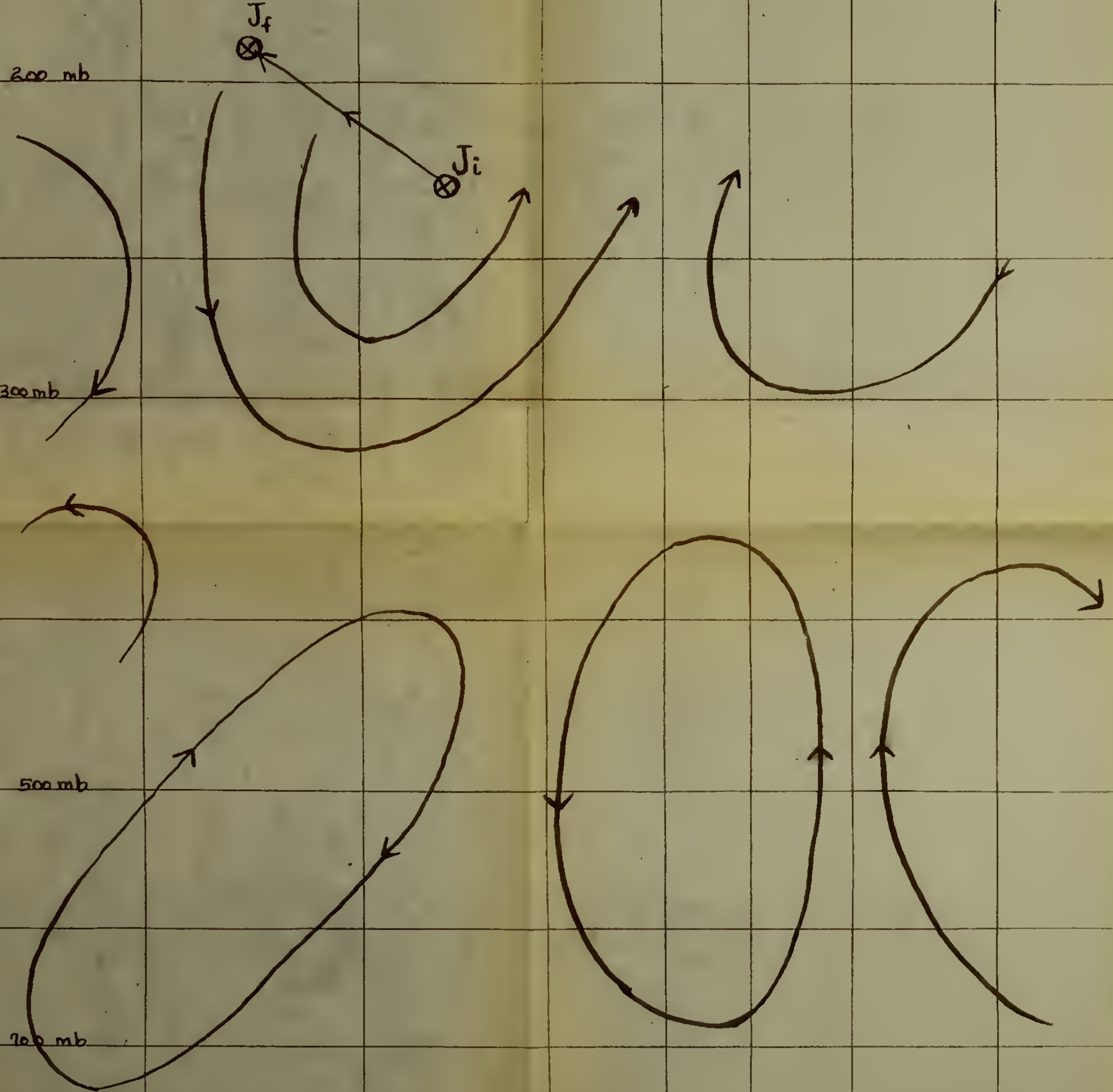


PLATE III

886
MOOSONEE

734
SAULT ST. MARIE

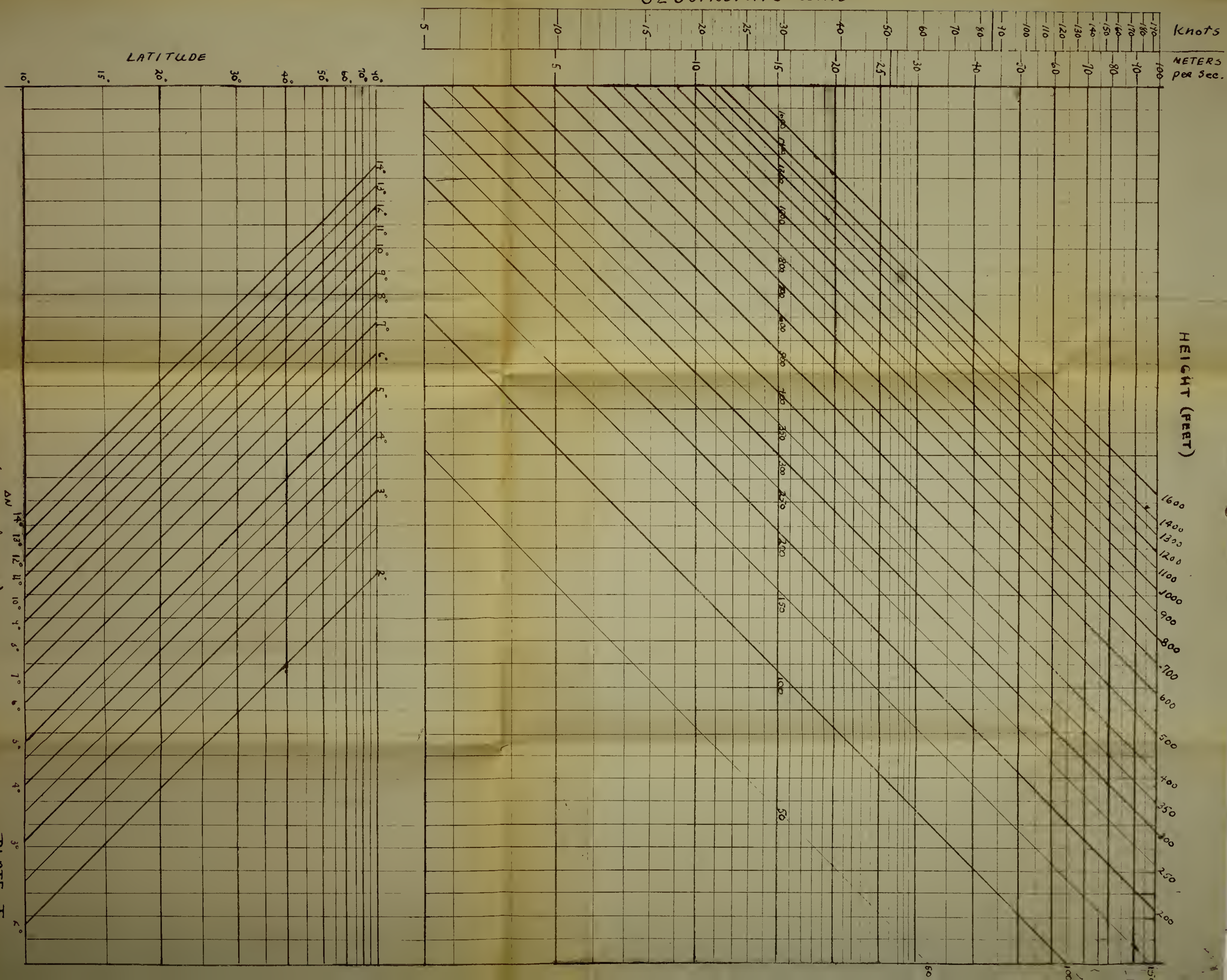
528
BUFFALO

520
PITTSBURGH HUNTINGTON GREENSBORO

425
CHARLESTON

NORTHWARD MOVING JET

22 Jan 1944 1500Z



GEOSTROPHIC WIND FROM SLOPE OF THE PRESSURE SURFACE

SPACING (DEGREES OF LATITUDE)

PLATE I

thesL16missing
Vertical motions and their relationship



C.1 3 2768 002 11255 9
DUDLEY KNOX LIBRARY